Hindawi
Geofluids
Volume 2022, Article ID 3637230, 15 pages
https://doi.org/10.1155/2022/3637230

Research Article

Approaches for Delineating Groundwater Recharge Potential Zone Using Fuzzy Logic Model

Mesfin Mamo Haile

Department of Hydraulic and Water Resources Engineering, Ambo University, Ambo, Ethiopia

Correspondence should be addressed to Mesfin Mamo Haile; mesfinmamo0355@gmail.com

Received 26 May 2022; Revised 29 September 2022; Accepted 29 October 2022; Published 14 November 2022

Academic Editor: Venkatramanan Senapathi

Groundwater recharge potential is an important spatial analysis to refer where the groundwater recharge is likely to happen. The present study discusses approaches for determining groundwater recharge potential zones in the Guder watershed, Ethiopia, using geospatial and fuzzy logic techniques on derived thematic layers based on significant influence of groundwater occurrence. A variety of thematic layers were created using satellite images and other ancillary data, including drainage density, slope, rainfall, geology, land use/land cover, lineament density, soil, and geomorphology. Researchers, expert opinion, and previous studies were used to estimate the membership value for each governing factors. According to the findings of the study, approximately 5.25% of the area has very high groundwater recharge potential, and 9.34% of the area has high groundwater recharge potential, while the areas with very low, low, and moderate groundwater recharge potential are approximately 20.04%, 34.21%, and 31.15%, respectively. The study's findings were confirmed by looking at the cross-tabulation area between the contributing features and the final map, which demonstrated strong associations. The findings of the study will help decision-makers and policymakers plan to implement appropriate groundwater recharge procedures. Fuzzy logic approaches have been found to be a basic tool for estimating groundwater recharge locations when used with GIS.

1. Introduction

Water is a critical input for agricultural production and plays an important role in food security. In Ethiopia, surface water is an important source of agricultural irrigation and drinking water. Farmers face a water shortage problem throughout the dry season (December–May) due to rising temperatures, which cause high evaporation and low rainfall levels; therefore, groundwater becomes an important additional freshwater supply. Groundwater is often a safe and dependable source of drinking water since it is less polluted than surface water [1–3]. Groundwater is constantly being used, depleted, and deteriorated as a result of rising population, agricultural activities, and rapid industrialisation. When rainfall infiltrates through the soil and reaches the aquifer, it significantly contributes to recharge the aquifer and enhance groundwater storage [4, 5].

Structures, topographic circumstances, lithological differences, slope gradients, soil, drainage form, and climate all influence groundwater availability and flow [6–8]. As a result, all of these factors must be addressed when assessing a region's groundwater recharge potential. Effective assessment of groundwater recharge requires precise scientific observations and cutting-edge techniques [9, 10]. Traditional in situ investigations of groundwater recharge potential are time-consuming and costly [11, 12]. Assessment of groundwater recharge potential zones has now become faster and more cost-effective as modern spatial techniques for hydrological applications have advanced in recent years [13].

Many researchers from across the world have performed groundwater potentiality evaluations using a combination of remote sensing and GIS approaches [14–22]. A precise mapping of groundwater recharge potential zones in typical basins might help with resourceful management of this critical source and reduce regional groundwater vulnerability [10, 23, 24]. As a result, an attempt was made in this study to determine groundwater recharge potential sites of the Guder watershed using GIS

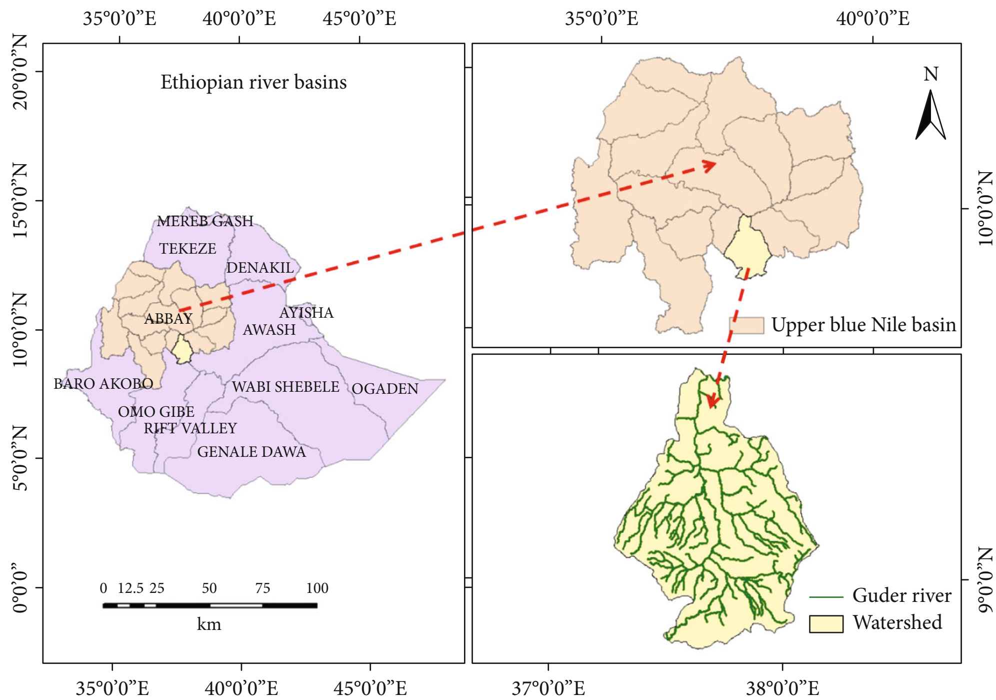

Figure 1: Guder subbasin map [25, 26].

and fuzzy logic approaches, as well as to compute the cross-relationship between the components and the final map, in preparation of a groundwater development plan. Fuzzy operators such as fuzzy sum, fuzzy product, and fuzzy Gamma are used for factor map integration. The fuzzy membership value created by map combination was used to divide the final groundwater recharge map into groups.

2. Description of the Study Area

The Guder subbasin is situated in Ethiopia's Oromia regional state, in the southern part of the Upper Blue Nile basin. The study's watershed is undulating, with elevations ranging from 934 m to 3323 m from the subbasin divide to the outlet. The watershed for the study was defined at the mouth of the Guder River, with areal coverage of 7011 km^2 and coordinates ranging from 7°30 to 9°30N latitudes and 37°00′ to 39°00′E longitudes (Figure 1). The Guder River's main tributaries are the Huluka, Tarantar, and Debis rivers.

3. Study Methodology

Figure 2 depicts the groundwater recharge potential mapping approach and techniques used. The topographic map and natural drainage lines were used to demarcate the study area base map, watershed, and subwatershed maps. The drainage density map was created in ArcGIS 10.5 using natural drain lines. The digital elevation model map was used to construct the slope and lineament density map, which was then used to calculate slope and validated with field triangulation points for greater accuracy. The resource maps based on ground data were utilized to create geomorphology, geology, and soil maps for the research region. The soil map was obtained from Ethiopia's Ministry of Water and Energy, and it has been updated using satellite imagery. The geology and geomorphology were compiled by the Geological Survey of Ethiopia (GSE) and were later updated with satellite imagery. The land use/land cover map was created using LANDSAT imagery and updated with satellite imagery from Google Earth Engine. For 30 years (1987–2017), the Ethiopian National Metrological Agency provided point precipitation records for the research region for 29 stations located in and around the Guder watershed. The ArcGIS 10.5 environment and the inverse distance weightage (IDW) interpolation method were used to construct the areal rainfall surface map. All thematic layers with 30 m pixel resolution were assigned UTM projection and WGS-1984 coordinate system and converted to raster format for overlay analysis using GIS software. The Jenks natural classification in the ArcGIS software was used to classify the overlaid maps based on groundwater recharge index values into separate groundwater recharge zone classes. To avoid bias in the output map, fuzzy logic is employed to specify the weightage of the feature layer. The obtained fuzzified value was assigned to thematic layers each class of respective topic based on fuzzy logic analysis. The membership value was assigned on a scale of 0-1, with 1 representing very strong recharge potential and 0 representing very low recharge potential. The recharge potential was divided into four categories: very low, low, moderate, high, and very high.

The fuzzy logic technique is interesting since it is simple to understand and apply. It can be utilized with data from any measurement scale, and the expert has complete control over the evidence weighing. The fuzzy logic paradigm enables more flexible weighted map combinations and is easy to implement when utilizing a GIS modelling software [27]. The evaluation

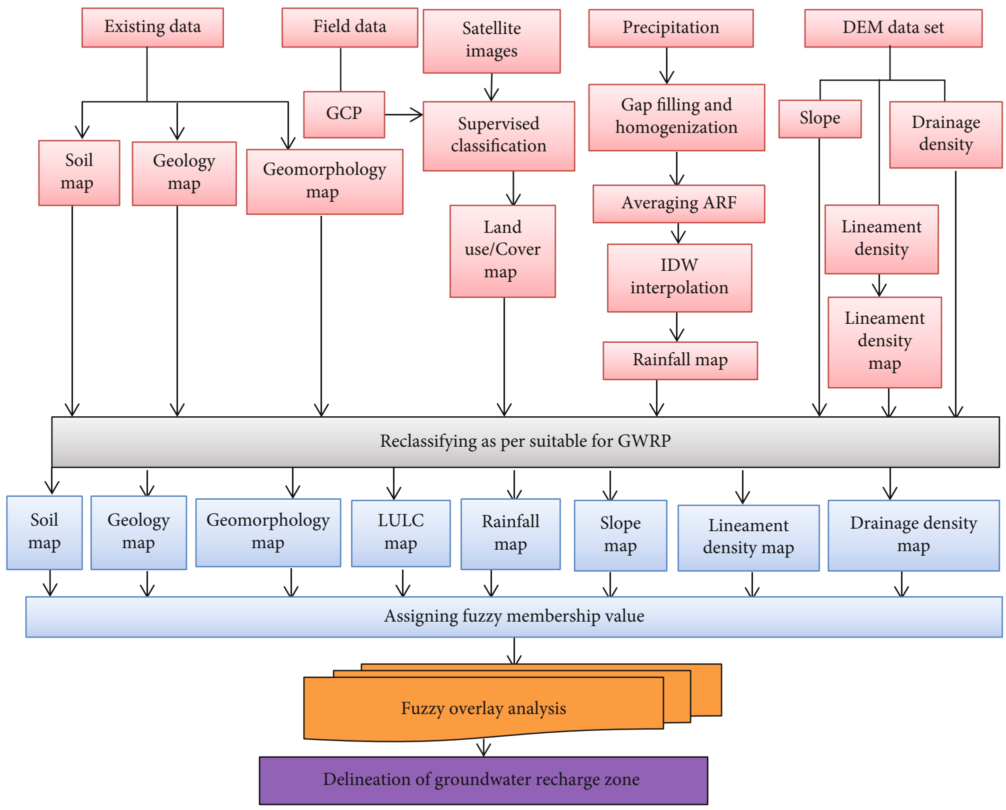

Figure 2: Flowchart for delineating the groundwater recharge potential zone.

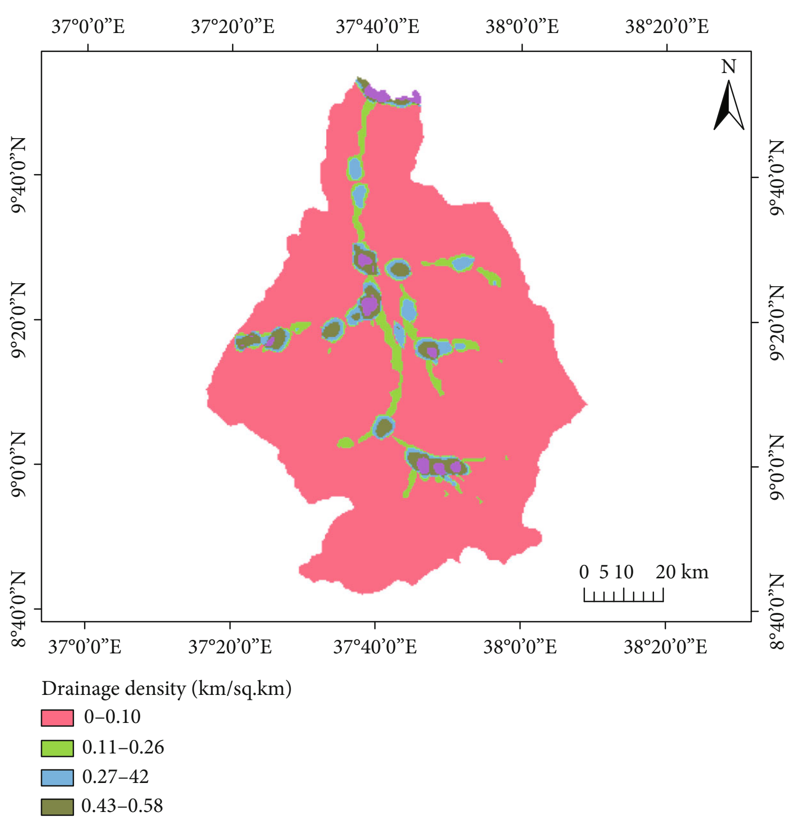

Figure 3: Drainage density of Guder watershed.

Table 1: Drainage density classes, membership value, and distribution.

Drainage density classes	GW recharge prospect	Membership value
0-0.10	Very high	0.88-1.0
0.11-0.26	High	0.51-0.88
0.27-0.42	Moderate	0.20-0.50
0.43-0.58	Low	0.072-0.20
0.59-0.96	Very low	0.072

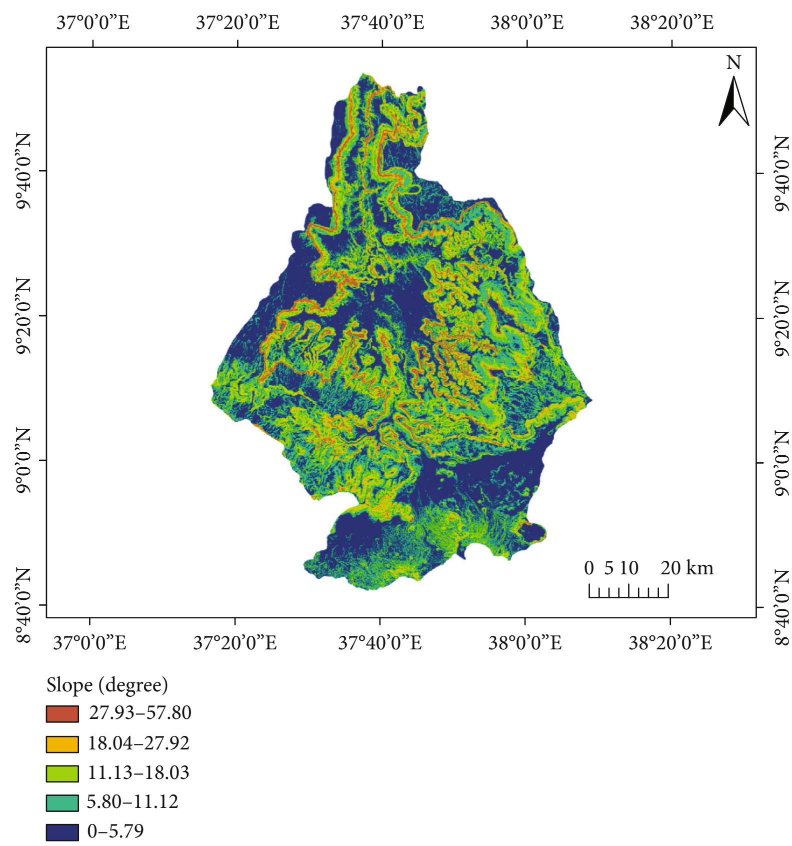

Figure 4: The slope of Guder watershed.

of fuzzy membership values is required for a fuzzy model to function properly [28]. The related value for each pixel (fuzzy membership value) in a fuzzy map illustrates the relative relevance of thematic layers as well as the relative values belonging to distinct parameters on the map region. Membership in fuzzy set theory can have any value between 0 and 1, expressing the level of certainty about a particular attribute of interest [29].

Several fuzzy operators are included in the fuzzy logic model, including fuzzy AND, fuzzy OR, fuzzy algebraic product, fuzzy algebraic sum, and fuzzy gamma [29]. These procedures are used to build factor maps based on the influence of thematic maps and the rank of parameters within each thematic. Because multiplying a large number by a small number generates a very small number of integrated fuzzified values at each site, the fuzzy algebraic product operator would be an excellent combination operator for identifying ideal locations for artificial recharging [30]. As a result, the fuzzy algebraic product was employed to identify erosion-prone areas in this

Table 2: Slope classes, membership value, and distribution.

Slope classes (%)	GW recharge prospect	Membership value
0-5.80	Very high	0.88-1.0
5.81-11.12	High	0.51-0.88
11.13-18.03	Moderate	0.21-0.51
18.03-27.92	Low	0.072-0.20
27.92-57.81	Very low	0.072

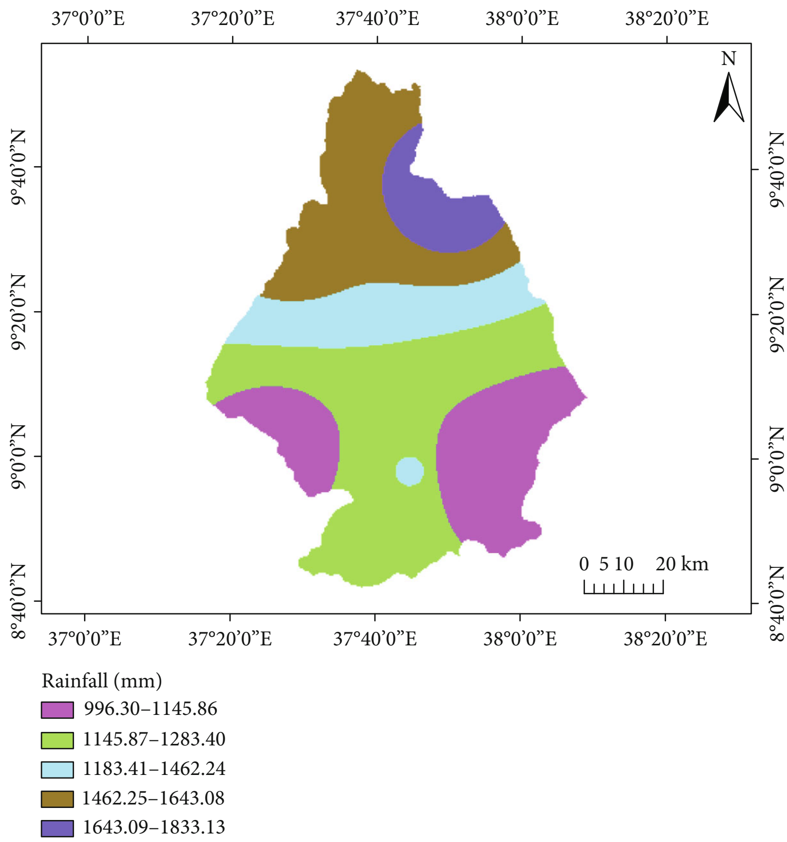

Figure 5: Rainfall map of the Guder watershed.

Table 3: Rainfall classes, membership value, and distribution.

Rainfall classes (mm)	GW recharge prospect	Membership value
996.30-1145.86	Very low	0.0041
1145.87-1283.39	Low	0.0041-0.12
1283.40-1462.24	Moderate	0.12-0.50
1462.25-1643.07	High	0.51-0.81
1643.08-1833.13	Very high	0.81-0.93

study. This is how the fuzzy algebraic product is determined:

$$\mu_{\text{combination}} = \prod_{i=1}^{n} \mu_i, \quad (1)$$

where μ_i is the ith map's fuzzy membership function.

The fuzzy membership has been assigned to the various thematic maps depending on their vulnerability to soil erosion (slope, land use, soil, rainfall, and topographic wetness index). Various experts have attributed weightage to different classes. Based on their rank, all expert weight has been converted into a fuzzified value ranging from 0 to 1. Fuzzy membership of parameters was performed using expert judgment and literature.

4. Result and Discussion

4.1. Drainage Density. Drainage density is calculated as a percentage of stream length per square kilometre [26]. It allows quantifying the possibility of surface runoff. There is a function for geology, geomorphology, rainfall, slope gradient, land utilization pattern, and vadose zone infiltration capability [30, 31]. Overland flow in the investigation area is disrupted by soil and bedrock physiognomies. The drainage density allows for a calculable analysis of the typical length of rivulet conduits stretching throughout the entire catchment area. The resulting map depicts a low-density area in the basin's center that gradually increases towards the basin's periphery. The density of drainage is classified as "very low" (0–0.10), "low" (0.11–0.26), "moderate" (0.27–0.42), "high" (0.43-0.58), and "very high" (0.59–0.10) (Figure 3). The greater density area has a membership value of 0.007 because it has a low recharge potential region, whereas the lower density area has a membership value of 0.88-1 because it has a larger probability of groundwater recharge (Table 1).

4.2. Slope. Slope impacts rainwater infiltration and overflow, making it an important consideration in groundwater recharge potential studies [32]. High slope areas have fast runoff and a short retention period to absorb water, resulting in a "very low" rate of groundwater recharge, whereas flat terrain has a longer retention period and hence a higher porosity and

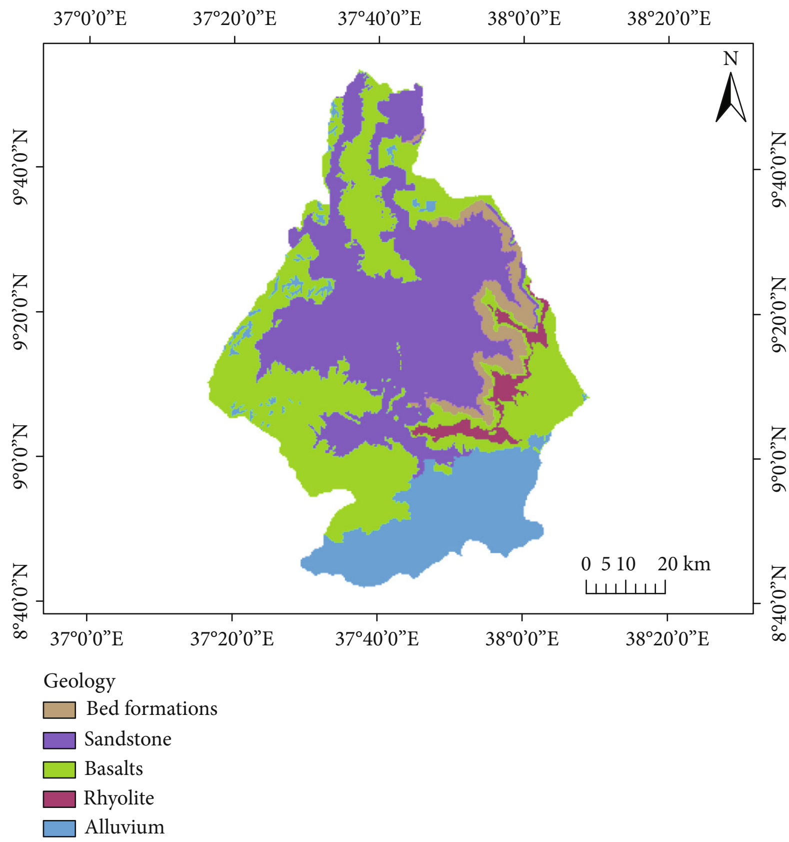

Figure 6: Geology of Guder watershed.

Table 4: Geology classes, membership value, and distribution.

Geology classes	GW recharge prospect	Membership value
Bed formation	Very low	0.041
Sandstone	Low	0.042-0.12
Basalt	Moderate	0.13-0.50
Rhyolite	High	0.51-0.81
Alluvium	Very high	0.82-0.93

permeability rate. A digital elevation model is reclassified into five slope classes to generate the slope map. Figure 4 shows the slope increasing from 0 to 57.8%. The fuzzy membership value of 0.072 is assigned to the high slope area established around the research area's edge of the water body, demonstrating less percolation, whereas flat terrain with 0–5.80% slope occupies the rest of the area. The majority of the area was found in flat terrain, which covered around 60% of the territory; as a result, the region is "very high" for groundwater recharge, with a fuzzy membership value of 0.88–1 (Table 2).

4.3. Rainfall. Rainfall affects the availability of water to seep into the subsurface and is directly tied to the capacity for groundwater recharge. The rainy season is concentrated in the study from June to September. For 30 years (1987–2017), the Ethiopian National Metrological Agency provided point precipitation records for the research region for 29 stations located in and around the Guder watershed. The inverse distance weighted (IDW) interpolation technique in the ArcGIS 10.5 was used to construct the areal rainfall map. Rainfall is influenced by the amount of rainfall. The yearly rainfall was measured in mm and categorized into five categories (Figure 5). The rainfall area with values less than 996.30–1145.86 mm will be assigned the fuzzified value of 0.0041, while the north part having rainfall more than 1462.24 mm is given the value of 0.51–1 (Table 3).

4.4. Geology. One of the most essential parameters in terms of groundwater recharge potential is the geological setting. Geological characteristics are significant for determining aquifer status, which indicates groundwater storage. Figure 6 depicts the basin's geological thematic map. The geological distribution of the research region is categorized into five classes depending on their potential to store groundwater. Bed formation is primarily made of gypsum and mud stone. There is lime stone intercalation at the bottom and shale intercalation at the top [19, 33]. It is a little too slightly weathered and compact. Mud stone, silt stone, and shale are the most common types of rocks in this formation. However, there are numerous beds with various intercalations. It has a high level of weathering. Fresh, large, and highly limited fracture surfaces result in very low permeability and limited groundwater occurrence. As a result, these rock formations are classed as being very

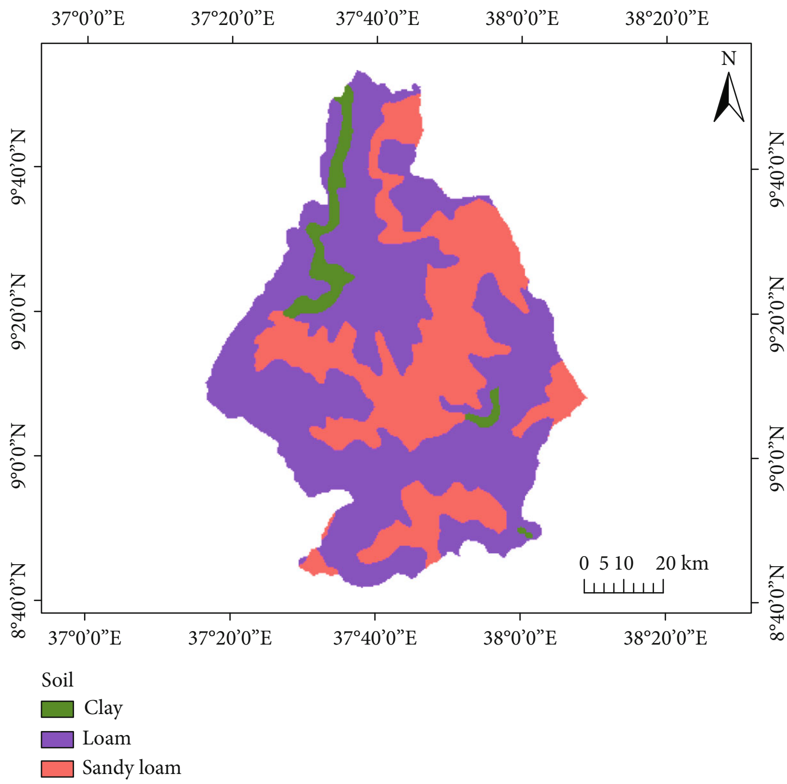

FIGURE 7: Soil type of the Guder watershed.

TABLE 5: Soil classes, membership value, and distribution.

Soil classes	GW recharge prospect	Membership value
Clay	Very low	0.03
Loam	Moderate	0.03-0.50
Sandy loam	High	0.50-0.88

unsuitable for groundwater recharge and have a fuzzified value of 0.041. Sandstone has both primary and secondary permeability when it comes to groundwater transport and occurrence. Its interstitial gaps make up the major water-bearing horizon. Furthermore, the occurrence and flow of groundwater is influenced by secondary cracks and joints, which increase porosity and permeability. However, precipitates from percolating water rapidly shut gaps in some places, reducing aquifer permeability. The bedding plains of sandstone in the research area are dipping towards the flow direction of rivers and gorges, and numerous springs follow this trend. Sandstones are often categorized as less favorable for groundwater recharge and have a fuzzy membership value of 0.0042–0.12. Basalt has a high secondary porosity and permeability. The unit's scoraceous lava flow nature is ideal for groundwater storage and circulation. The permeability is greatly dependent on the degree and depth of fracture, and the formation of joints on basalt offers the aquifer good hydraulic properties. With a diverse mode of occurrence, central volcanic basalts have good water holding qualities. Because of their vesicular shape and boulder-forming features, they are an excellent aquifer with high groundwater occurrence and movement. The vesicles, on the other hand, are packed with secondary components, and the weathering process gives them a relatively high permeability. This unit consists of domes and hills that have little groundwater availability but serve as an excellent recharge region for the underlying aquifer [33]. As a result, this formation was classified as fairly appropriate for groundwater recharge and given a fuzzified value of 0.13-0.5. Rhyolite geological units generate steep slope ridges and flat terrain that is largely confined. It is heavily weathered on top and big and fresh on the bottom. However, vertically formed fractures are occasionally observed in rhyolite and trachyte interlayers. It is made up of ignimbrites and subordinate trachytes. These formations are awarded a fuzzified value of 0.51–0.81 and are classified as highly favorable for groundwater recharge. Alluvium is a significant source of shallow groundwater. Because the texture ranges from sand to coarse gravel with loose and undifferentiated grains, it has relatively good permeability and productivity. The majority of the alluvial sediments are recharged by infiltration from perennial rivers and streams. The grains of the sediments demonstrate poor sorting in some regions, resulting in very low productivity. As a result, the geological class is classified as very highly suited for groundwater recharge zone with a fuzzified value of 0.82–1 (Table 4).

4.5. Soil. Soil plays a major role in groundwater recharge [3, 34, 35]. The soil survey map and field study classify the area as sandy loam, loam, and clay (Figure 7). The soil texture in

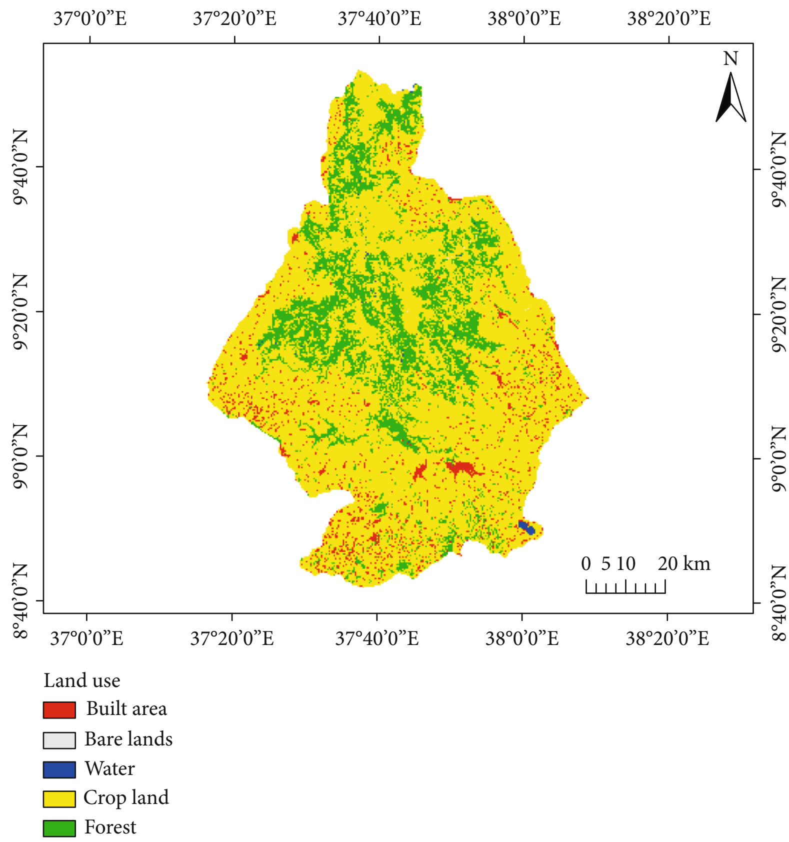

Figure 8: Land use of the Guder watershed.

Table 6: Geology classes, membership value, and distribution.

Geology classes	GW recharge prospect	Membership value
Trees	Very high	0.88-1.0
Crop land	High	0.51-0.88
Water	Moderate	0.19-0.50
Bare land	Low	0.073-0.20
Built area	Very low	0.072

Table 7: Lineament density classes, membership value, and distribution.

Lineament classes	GW recharge prospect	Membership value
0-0.31	Very low	0.0041
0.32–0.90	Low	0.0041-0.11
0.91–1.72	Moderate	0.12-0.50
1.73–3.38	High	0.50-0.80
3.38-7.33	Very high	0.80-0.93

the majority of the studied areas is loam or sandy loam. Sandy loam soil has a high infiltration rate due to its strong perviousness and penetrability [33] and has been assigned the highest priority and fuzzy membership value of 0.51-0.88. Clay soil has a low priority membership value of 0.03 because it is compacted and impermeable (Table 5).

4.6. Land Use/Land Cover. Because it influences overland flow, evapotranspiration, infiltration, and aquifer system repair, land use is an effective predictor of hydrogeological changes in the water cycle [36, 37]. The map was built by obtaining a Landsat satellite image from Google Earth Engine land use 2020 (Sentinel-2) and classifying it with the ERDAS Imagine 2016 stratified supervised classification algorithm. The basic land use class categories are crop land, barren land, forest, built-up area, and water bodies (Figure 8). Forest and agriculture land create modest overland flow [38], making it "very high" for groundwater recharge and assigned a fuzzified value of 0.51–1. Built-up region, on the other hand, percolates less water and hence has a membership value of 0.072 as a site with very low groundwater recharge potential (Table 6).

4.7. Lineament Density. Lineaments are tectonic linear, rectilinear, and curvilinear features visible in satellite imagery [39], and they can classify master joints, fractures, faults, topographic linearity and formation, vegetation cover, infrastructure such as roads and bridges, valleys, and stream straight courses, and boundaries between different lithological units [40]. Lineaments were retrieved from the research area's digital elevation model, and additional editing and watershed categorization work was conducted in the ArcGIS spatial analyst tool environment. High

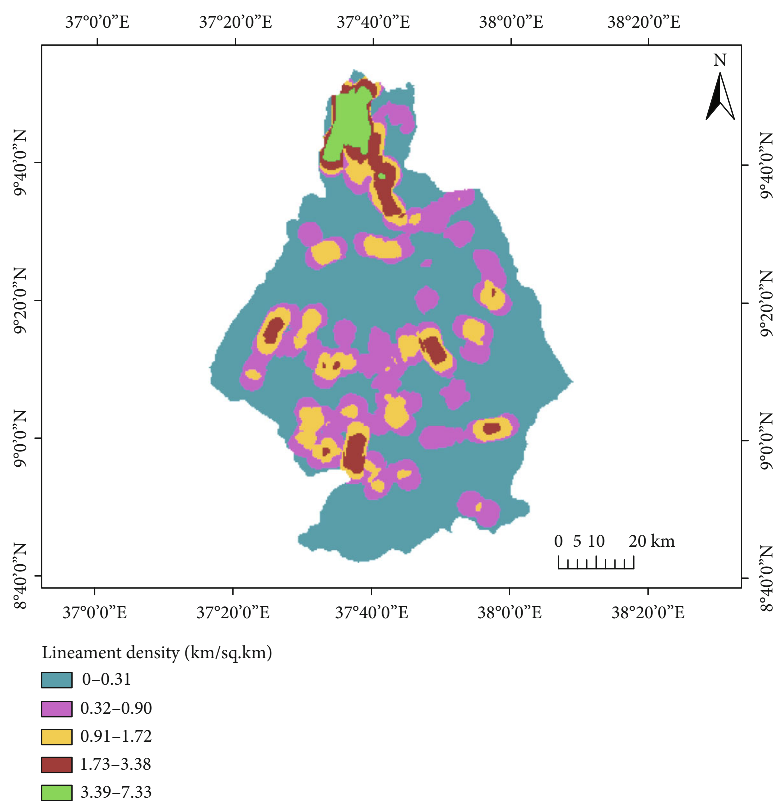

Figure 9: Lineament density map of Guder watershed.

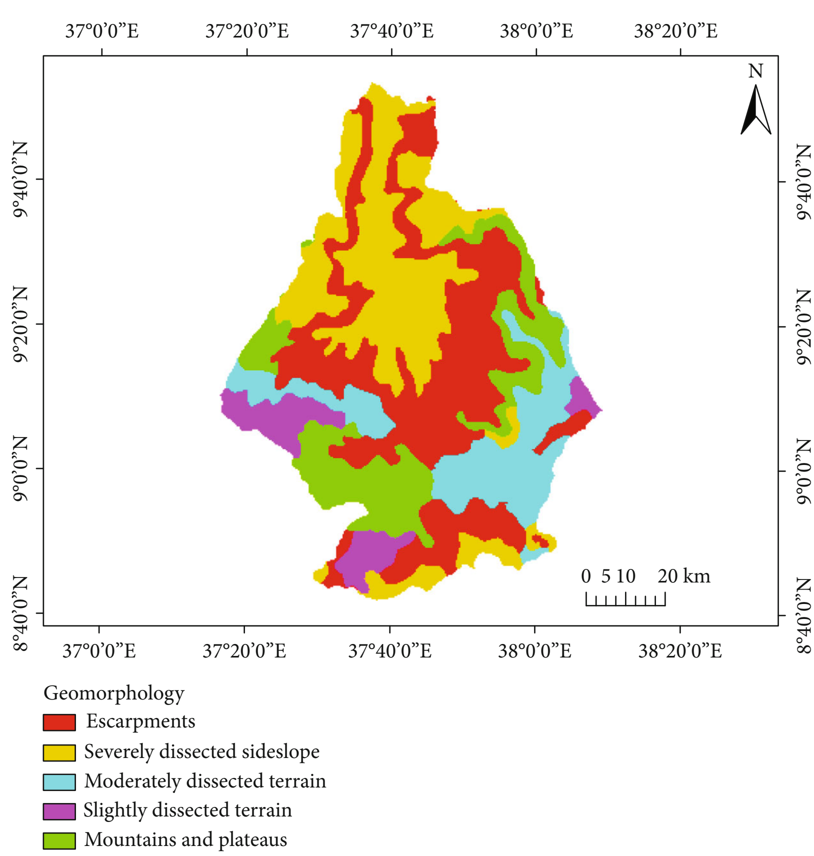

Figure 10: Geomorphology of the Guder watershed.

Table 8: Geomorphology classes, membership value, and distribution.

Geomorphology classes	GW recharge prospect	Membership value
Escarpments	Very low	0.0041
Severely dissected terrain	Low	0.0041-0.12
Moderately dissected terrain	Moderate	0.13-0.50
Slightly dissected terrain	High	0.51-0.80
Mountains and plateaus	Very high	0.80-1.0

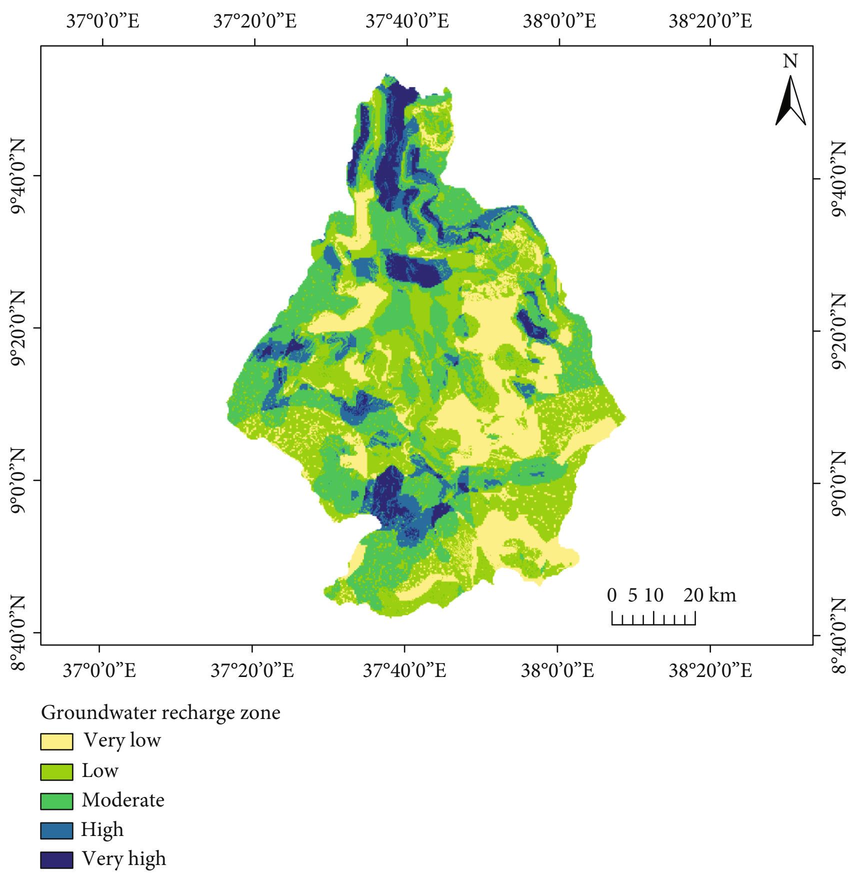

Figure 11: Groundwater recharge zones of the study area.

Table 9: Groundwater recharges classes, membership value, and distribution.

GWR prospect	Membership value	Areal coverage (sq.km)	Coverage (%)
Very low	0.00-0.20	1399	20.04
Low	0.20-0.27	2388	34.21
Moderate	0.28-0.50	2174	31.15
High	0.51-0.8	652	9.34
Very high	0.8-1	367	5.26

Table 10: Cross-tabulation between GWR and drainage density.

GWR/ drainage density	0.59-0.96	0.43-0.58	0.27-0.42	0.11-0.26	0-0.10
Very low	1375.71	17.22	5.01	1.16	0.00
Low	2258.72	81.79	28.46	14.12	4.91
Moderate	1805.88	151.14	96.79	82.99	37.04
High	541.76	27.61	28.31	40.72	13.83
Very high	215.38	43.08	41.57	43.40	23.99

Table 11: Cross-tabulation between GWR and slope.

GWR/slope	27.92-57.81	18.03-27.92	11.13-18.03	5.81-11.12	0-5.80
Very low	98.08	214.85	371.22	397.55	316.75
Low	106.50	226.68	437.66	761.97	855.16
Moderate	39.60	105.73	316.50	660.71	1050.29
High	19.52	74.54	130.28	204.55	224.06
Very high	4.27	20.22	57.83	124.37	160.81

Table 12: Cross-tabulation between GWR and rainfall.

GWR/rainfall	996.30-1145.86	1145.87-1283.39	1283.40-1462.24	1462.25-1643.07	1643.08-1833.13
Very low	522.82	441.79	223.13	183.81	30.39
Low	735.82	875.68	289.86	204.36	22.34
Moderate	267.81	820.87	349.14	384.59	110.22
High	14.45	259.92	94.73	508.97	81.63
Very high	0.00	91.60	34.56	217.92	237.73

Table 13: Cross-tabulation between GWR and geology.

GWR/geology	Bed formation	Sandstone	Basalt	Rhyolite	Alluvium
Very low	179.62	623.75	242.32	6.70	29.79
Low	88.32	1150.40	545.41	7.60	21.30
Moderate	65.09	699.26	1081.29	52.13	284.62
High	1.04	205.24	411.81	56.45	302.49
Very high	0.00	27.40	309.94	54.96	556.58

Table 14: Cross-tabulation between GWR and soil.

GWR/soil	Clay	Loam	Sandy loam
Very low	167.72	511.80	722.41
Low	76.56	1304.51	332.76
Moderate	44.83	532.50	466.22
High	2.38	1673.46	120.20
Very high	0.00	33.66	1015.10

Table 15: Cross-tabulation between GWR and land use.

GWR/land use	Built area	Bare land	Water	Crop land	Forest
Very low	132.12	0.60	8.04	912.18	349.29
Low	125.42	1.79	2.53	1715.02	551.12
Moderate	34.56	0.60	3.28	1825.25	320.99
High	17.87	0.00	0.30	526.39	110.67
Very high	0.00	0.00	0.89	300.73	64.79

Table 16: Cross-tabulation between GWR and lineament density.

GWR/lineament density	0-0.31	0.32–0.90	0.91–1.72	1.73–3.38	3.38-7.33
Very low	1258.79	125.71	15.49	0.60	1.34
Low	1583.05	581.95	168.76	37.39	25.02
Moderate	1325.07	469.20	262.60	85.20	42.45
High	57.64	345.72	137.78	77.45	36.49
Very high	4.92	63.45	145.53	93.84	58.69

Table 17: Cross-tabulation between GWR and geomorphology.

GWR/ geomorphology	Escarpments	Severely dissected terrain	Moderately dissected terrain	Slightly dissected terrain	Mountains and plateaus
Very low	1046.98	122.88	71.05	40.66	120.35
Low	961.93	800.46	447.00	225.66	218.36
Moderate	329.48	543.22	375.51	203.17	107.99
High	4.02	48.41	109.63	271.24	221.79
Very high	0.00	232.66	25.17	0.60	475.90

lineament densities are preferable for groundwater recharging. As a result, high-density lineaments have a high fuzzified value, while low-density lineaments have a low fuzzified value (Table 7). The map was finished when lineament density was determined, and it was classed into five groups (Figure 9).

4.8. Geomorphology. Geomorphological research illuminates topography, landforms, and the drainage network. Weathering, erosion, and deposition have all contributed to the formation of diverse landforms in the area's upstream and downstream regions [41]. The basin's multiple geomorphic units are described as mountainous area, somewhat dissected terrain, severely dissected terrain, and escarpment (Figure 10). Mountainous terrain is awarded a fuzzy membership value of 0.8-1, while mildly and moderately dissected terrain is assigned a fuzzy membership value of 0.51-0.8 and 0.13-0.50, respectively. Due to basaltic rock exposure, the severely dissected topography and escarpments generate significant surface runoff, thin soil cover, steep slopes, and sparse vegetation, leading in a limited groundwater recharge capacity, and are awarded membership values of 0.041–0.12 and 0.041, respectively (Table 8).

4.9. Groundwater Recharge Zone Mapping. Each thematic layer was converted to a raster file, and appropriate fuzzy membership values were assigned using the fuzzy membership function in a GIS environment. The final output of the fuzzy logic overlay indicates the optimum groundwater recharge potential sites based on the combined input fuzzy membership values (Figure 11). The fuzzy logic overlay result for groundwater recharge was further divided into five categories: very high, high, moderate, low, and very low groundwater recharge suitable location. Table 9 demonstrates how zonal statistics were used to calculate the area of each of the five fuzzy membership values.

4.10. Cross-Tabulation between Groundwater Recharge Area and Contributing Factors. The association between groundwater recharge area and factors involved has been determined using cross-tabulation.

4.11. Cross-Tabulation between GWR and Drainage Density. One of the factors considered in groundwater recharge study was drainage density, and the cross-tabulation outcomes with groundwater recharge locations are displayed in Table 10. The results showed that majority of very low and low groundwater zones were observed in high drainage density area (0.27–0.96 km/sq.km). In contrast, majority of low drainage density areas (0–0.26 km/sq.km) were home for very high and high groundwater recharge potential zones.

4.12. Cross-Tabulation between GWR and Slope. The relationship between groundwater recharge zone and slope was found by cross-tabulating final map of groundwater recharge zone with the slope of the study area. The results (Table 11) showed that very high and high groundwater zones were observed in gentle step slopes of 0-11%. In contrast, steeply step slope zones have very low and low groundwater recharge potential zones.

4.13. Cross-Tabulation between GWR and Rainfall. The groundwater recharge study included rainfall as an additional factor, and the cross-tabulation outcomes with groundwater recharge locations are displayed in Table 12. According to the cross-tabulation results, the majority of the very high and high groundwater recharge potential zones were situated in areas with very high and high rainfall. Alternatively, sites with very low and low rainfall displayed very low and low groundwater recharge zones, respectively.

4.14. Cross-Tabulation between GWR and Geology. Geology was considered as the main factors which impacts the groundwater recharge zones. Its relationship with groundwater recharge zone was determined by cross-tabulating final map of groundwater recharge zone with the geology of the study area. The results (Table 13) showed that very high and high groundwater zones were observed in bed, sandstone, and basalt formations. In contrast, rhyolite and alluvium were highly suitable for groundwater recharge potential zones.

4.15. Cross-Tabulation between GWR and Soil. From cross-tabulation result, 1673.46 km^2 and 1015.10 km^2 area of the Guder watershed were high, and very high groundwater recharge potential areas were found in loam and sandy loam soil textures (Table 14). The majority of clay areas were less suitable for groundwater recharge zone.

4.16. Cross-Tabulation between GWR and Land Use. The effects of land cover on groundwater recharge potential were demonstrated using cross-tabulation in the ArcGIS model. Forest and crop land were home to the majority of the very high and high groundwater recharge potential zones, according to the cross-tabulation data. The majority of built area and bare land locations, on the other hand, exhibited very low and low groundwater recharge responses, respectively (Table 15).

4.17. Cross-Tabulation between GWR and Lineament Density. The relationship between groundwater recharge zone and lineament density was determined by cross-tabulating final map of groundwater recharge zone with the lineament density map of the study area. The results (Table 16) showed that very low and low groundwater zones were observed in less lineament density of 0–0.9 km/sq.km. In contrast, higher lineament density (1.73–7.33 km/sq.km) zones were home for very high and high groundwater recharge potential zones.

4.18. Cross-Tabulation between GWR and Geomorphology. The relationship between groundwater recharge zone and geomorphology was found by cross-tabulating final map of groundwater recharge zone with the geomorphology map of the study area. The results (Table 17) showed that very high and high groundwater zones were observed in slightly dissected terrain and mountainous area. In contrast, escarpments and severely dissected terrain zones have very low and low groundwater recharge potential zones.

5. Conclusion

The current work offers a method for identifying groundwater recharge potential zones for water management strategies and artificial recharge to aquifers in Guder watershed, Ethiopia. Water resource extension is accomplished by assessing available recharge space for recharge as well as subwatershed wise deficient or surplus surface water availability to conserve in artificial recharge structures. About 5.25% of the research area has very high groundwater recharge potential, whereas 9.34% has moderate groundwater recharge potential. The remaining 20.04%, 34.21%, and 31.15% of the total area fall into the very low, low, and moderate groundwater recharge potential zones, respectively. The cross-tabulation investigations show that the groundwater recharge potential zone map is actually accurate and provides valuable inputs for resource management. The application of MCDA analysis attests to the improved accuracy. Thus, remote sensing, GIS, and fuzzy logic techniques have outperformed other conventional techniques in identifying suitable sites for groundwater recharging. The same appropriate methods were recommended for complex areas to delineate groundwater potential and recharge zone in the small area. The groundwater recharge potential map along with other thematic map forms serves as resource information database that can be updated from time to time by adding new information. In this research, integrated GIS and AHP techniques are very useful, time, and cost-effective tool for the identification and delineation of groundwater potential and recharge zones and analysis.

Data Availability

The datasets generated during and/or analysed during this study are available from the corresponding author on reasonable request.

Conflicts of Interest

The author declares no conflict of interest.

References

[1] N. Adimalla, "Groundwater quality for drinking and irrigation purposes and potential health risks assessment: a case study from semi-arid region of South India," *Exposure Health*, vol. 11, no. 2, pp. 109–123, 2018.

[2] A. K. Kadam, V. M. Wagh, A. A. Muley, B. N. Umrikar, and R. N. Sankhua, "Prediction of water quality index using artificial neural network and multiple linear regression modelling approach in Shivganga River basin, India," *Modeling Earth Systems and Environment*, vol. 5, no. 3, pp. 951–962, 2019.

[3] S. Patra, P. Mishra, and S. C. Mahapatra, "Delineation of groundwater potential zone for sustainable development: a case study from Ganga Alluvial Plain covering Hooghly district of India using remote sensing, geographic information system and analytic hierarchy process," *Journal of Cleaner Production*, vol. 172, pp. 2485–2502, 2018.

[4] M. Rajasekhar, G. S. Raju, R. S. Raju, and U. I. Basha, "Data on artificial recharge sites identified by geospatial tools in semi-arid region of Anantapur district, Andhra Pradesh, India," *Data in Brief*, vol. 19, pp. 462–474, 2018.

[5] H.-F. Yeh, Y.-S. Cheng, H.-I. Lin, and C.-H. Lee, "Mapping groundwater recharge potential zone using a GIS approach in Hualian river, Taiwan," *Sustainable Environment Research*, vol. 26, no. 1, pp. 33–43, 2016.

[6] A. Adham, K. N. Sayl, R. Abed et al., "A GIS-based approach for identifying potential sites for harvesting rainwater in the Western Desert of Iraq," *International Soil and Water Conservation Research*, vol. 6, no. 4, pp. 297–304, 2018.

[7] S. Mishra, D. Tiwary, A. Ohri, and A. K. Agnihotri, "Impact of municipal solid waste landfill leachate on groundwater quality in Varanasi, India," *Groundwater for Sustainable Development*, vol. 9, no. 10, pp. 100230–101030, 2019.

[8] I. P. Senanayake, D. M. D. O. K. Dissanayake, B. B. Mayadunna, and W. L. Weerasekera, "An approach to delineate groundwater recharge potential sites in Ambalantota, Sri Lanka using GIS techniques," *Geoscience Frontiers*, vol. 7, no. 1, pp. 115–124, 2016.

[9] N. S. Magesh, N. Chandrasekar, and J. P. Soundranayagam, "Delineation of groundwater potential zones in Theni district, Tamil Nadu, using remote sensing, GIS and MIF techniques," *Geoscience frontiers*, vol. 3, no. 2, pp. 189–196, 2012.

[10] M. Rajasekhar, S. R. Gadhiraju, A. Kadam, and V. Bhagat, "Identification of groundwater recharge-based potential rainwater harvesting sites for sustainable development of a semiarid region of southern India using geospatial, AHP, and SCS-CN approach," *Arabian Journal of Geosciences*, vol. 13, no. 1, p. 24, 2020.

[11] I. Chenini and A. B. Mammou, "Groundwater recharge study in arid region: an approach using GIS techniques and numerical modeling," *Computational Geosciences*, vol. 36, no. 6, pp. 801–817, 2010.

[12] S. Deepa, S. Venkateswaran, R. Ayyandurai, R. Kannan, and M. J. Prabhu, "Groundwater recharge potential zones mapping in upper Manimuktha sub basin Vellar River Tamil Nadu India using GIS and remote sensing techniques," *Modeling Earth Systems and Environment*, vol. 2, no. 3, p. 137, 2016.

[13] S. Owusu, M. L. Mul, B. Ghansah, P. K. Osei-Owusu, V. Awotwe-Pratt, and D. Kadyampakeni, "Assessing land suitability for aquifer storage and recharge in northern Ghana using remote sensing and GIS multi-criteria decision analysis technique," *Modeling Earth Systems and Environment*, vol. 3, no. 4, pp. 1383–1393, 2017.

[14] A. Singhai, S. Das, A. K. Kadam, J. P. Shukla, D. S. Bundela, and M. Kalashetty, "GIS-based multi-criteria approach for identification of rainwater harvesting zones in upper Betwa sub-basin of Madhya Pradesh, India," *Environment, Development and Sustainability*, vol. 21, no. 2, pp. 777–797, 2019.

[15] M. A. Jenifer and M. K. Jha, "Comparison of analytic hierarchy process, catastrophe and entropy techniques for evaluating groundwater prospect of hard-rock aquifer systems," *Journal of Hydrology*, vol. 548, pp. 605–624, 2017.

[16] U. Mandal, S. Sahoo, S. B. Munusamy et al., "Delineation of groundwater potential zones of coastal groundwater basin using multi-criteria decision making technique," *Water Resources Management*, vol. 30, no. 12, pp. 4293–4310, 2016.

[17] S. A. Naghibi, H. R. Pourghasemi, Z. S. Pourtaghi, and A. Rezaei, "Groundwater qanat potential mapping using frequency ratio and Shannon's entropy models in the Moghan watershed, Iran," *Earth Science Informatics*, vol. 8, no. 1, pp. 171–186, 2015.

[18] L. K. Singh, M. K. Jha, and V. M. Chowdary, "Multi-criteria analysis and GIS modeling for identifying prospective water harvesting and artificial recharge sites for sustainable water supply," *Journal of Cleaner Production*, vol. 142, pp. 1436–1456, 2017.

[19] M. M. Haile, J. Tafesse Yadeta, and L. Amena Gambe, "Delineation of groundwater potential zones using geo-spatial and AHP techniques: Ambo area, Blue Nile Basin, Ethiopia," *Sustainable Water Resources Management*, vol. 8, no. 1, p. 36, 2022.

[20] S. Barua, B. P. Mukhopadhyay, and A. Bera, "Integrated assessment of groundwater potential zone under agricultural dominated areas in the western part of Dakshin Dinajpur district, West Bengal, India," *Arabian Journal of Geosciences*, vol. 14, no. 11, p. 1042, 2021.

[21] A. Bera, B. P. Mukhopadhyay, and S. Barua, "Delineation of groundwater potential zones in Karha river basin, Maharashtra, India, using AHP and geospatial techniques," *Arabian Journal of Geosciences*, vol. 13, no. 15, p. 693, 2020.

[22] S. Biswas, B. P. Mukhopadhyay, and A. Bera, "Delineating groundwater potential zones of agriculture dominated landscapes using GIS based AHP techniques: a case study from Uttar Dinajpur district, West Bengal," *Environmental Earth Sciences*, vol. 79, no. 12, p. 302, 2020.

[23] F. K. Zaidi, Y. Nazzal, I. Ahmed, M. Naeem, and M. K. Jafri, "Identification of potential artificial groundwater recharge zones in northwestern Saudi Arabia using GIS and Boolean logic," *Journal of African Earth Sciences*, vol. 111, pp. 156–169, 2015.

[24] S. Kaliraj, N. Chandrasekar, and N. S. Magesh, "Identification of potential groundwater recharge zones in Vaigai upper basin, Tamil Nadu, using GIS-based analytical hierarchical process (AHP) technique," *Arabian Journal of Geosciences*, vol. 7, no. 4, pp. 1385–1401, 2014.

[25] M. M. Haile, "Application of geospatial technology coupled with fuzzy logic operations in mapping soil-erosion critical zones: the case of Guder sub-basin, upper Blue Nile Basin, Ethiopia," *Applied Water Science*, vol. 12, no. 8, p. 195, 2022.

[26] M. M. Haile and A. K. Abebe, "GIS and fuzzy logic integration in land suitability assessment for surface irrigation: the case of Guder watershed, Upper Blue Nile Basin, Ethiopia," *Applied Water Science*, vol. 12, no. 10, p. 240, 2022.

[27] B. Pradhan, S. Lee, and M. F. Buchroithner, "Use of geospatial data and fuzzy algebraic operators to landslide-hazard mapping," *Applied Geomatics*, vol. 1, no. 1-2, pp. 3–15, 2009.

[28] S. Ebadi, J. Valadanzoej, and A. Vafacinezhad, *Evaluation of Indexing Overlay, Fuzzy Logic and Genetic Algorithm Method for Industrial Estate Site Selection in GIS Environment*, Tehran, Iran, 2001.

[29] M. H. Tangestani, "Landslide susceptibility mapping using the fuzzy gamma operation in a GIS, Kakan catchment area, Iran," in *The 6th annual International conference Map India*, Newdelhi, India, January 2003.

[30] M. M. Saravi, A. Malekian, and B. Nouri, "Identification of suitable sites for groundwater recharge," in *The 2nd International Conference on Water Resources and Arid Environment*, Riyadh, Saudi Arabia, November, 2006.

[31] R. E. Horton, "Drainage basin characteristics," *Transactions of the American Geophysical Union*, vol. 13, no. 1, pp. 350–361, 1932.

[32] R. Bali, K. Agarwal, S. Nawaz Ali, S. Rastogi, and K. Krishna, "Drainage morphometry of Himalayan Glacio-fluvial basin, India: hydrologic and neotectonic implications," *Environment and Earth Science*, vol. 66, no. 4, pp. 1163–1174, 2012.

[33] G. Shailaja, A. K. Kadam, G. Gupta, B. N. Umrikar, and N. J. Pawar, "Integrated geophysical, geospatial and multiple-criteria decision analysis techniques for delineation of groundwater potential zones in a semi-arid hard-rock aquifer in Maharashtra, India," *Hydrogeology Journal*, vol. 27, no. 2, pp. 639–654, 2019.

[34] A. K. Kadam, S. S. Kale, N. N. Pande, N. J. Pawar, and R. N. Sankhua, "Identifying potential rainwater harvesting sites of a semi-arid, basaltic region of Western India, using SCS-CN method," *Water Resources Management*, vol. 26, no. 9, pp. 2537–2554, 2012.

[35] S. Kebede, A. Hailu, E. Crane, Ó. D. BÉ, and I. Bellwood-Howard, *Africa Groundwater Atlas: Hydrogeology of Ethiopia*, British Geological Survey, Nottingham, 2018.

[36] R. Umar, I. Ahmed, and F. Alam, "Mapping groundwater vulnerable zones using modified DRASTIC approach of an alluvial aquifer in parts of central Ganga plain, Western Uttar Pradesh," *Journal of the Geological Society of India*, vol. 73, no. 2, pp. 193–201, 2009.

[37] A. K. Kadam, S. S. Kale, B. N. Umrikar, R. N. Sankhua, and N. J. Pawar, "Identifying possible locations to construct soil water conservation structures by using hydrogeological and geospatial analysis," *Hydrospatial Analysis*, vol. 1, no. 1, pp. 18–27, 2017.

[38] A. K. Kadam, B. N. Umrikar, and R. N. Sankhua, "Assessment of recharge potential zones for groundwater development and management using geospatial and MCDA technologies in semiarid region of Western India," *SN Applied Sciences*, vol. 2, no. 2, p. 312, 2020.

[39] S. Selvam and P. Sivasubramanian, "Groundwater potential zone identification using geoelectrical survey: a case study from Medak district, Andhra Pradesh, India," *International Journal of Geomatics and Geosciences*, vol. 3, no. 1, pp. 55–62, 2012.

[40] T. Kumar, A. K. Gautam, and T. Kumar, "Appraising the accuracy of GIS-based multi-criteria decision making technique for delineation of groundwater potential zones," *Water Resources Management*, vol. 28, no. 13, pp. 4449–4466, 2014.

[41] K. G. Berhanu and S. D. Hatiye, "Identification of groundwater potential zones using proxy data: case study of Megech watershed, Ethiopia," *Journal of Hydrology: Regional Studies*, vol. 28, article 100676, 2020.